Open-File Report 91-502

GEOMORPHIC AND VEGETATIVE RECOVERY PROCESSES ALONG MODIFIED STREAM CHANNELS OF WEST TENNESSEE

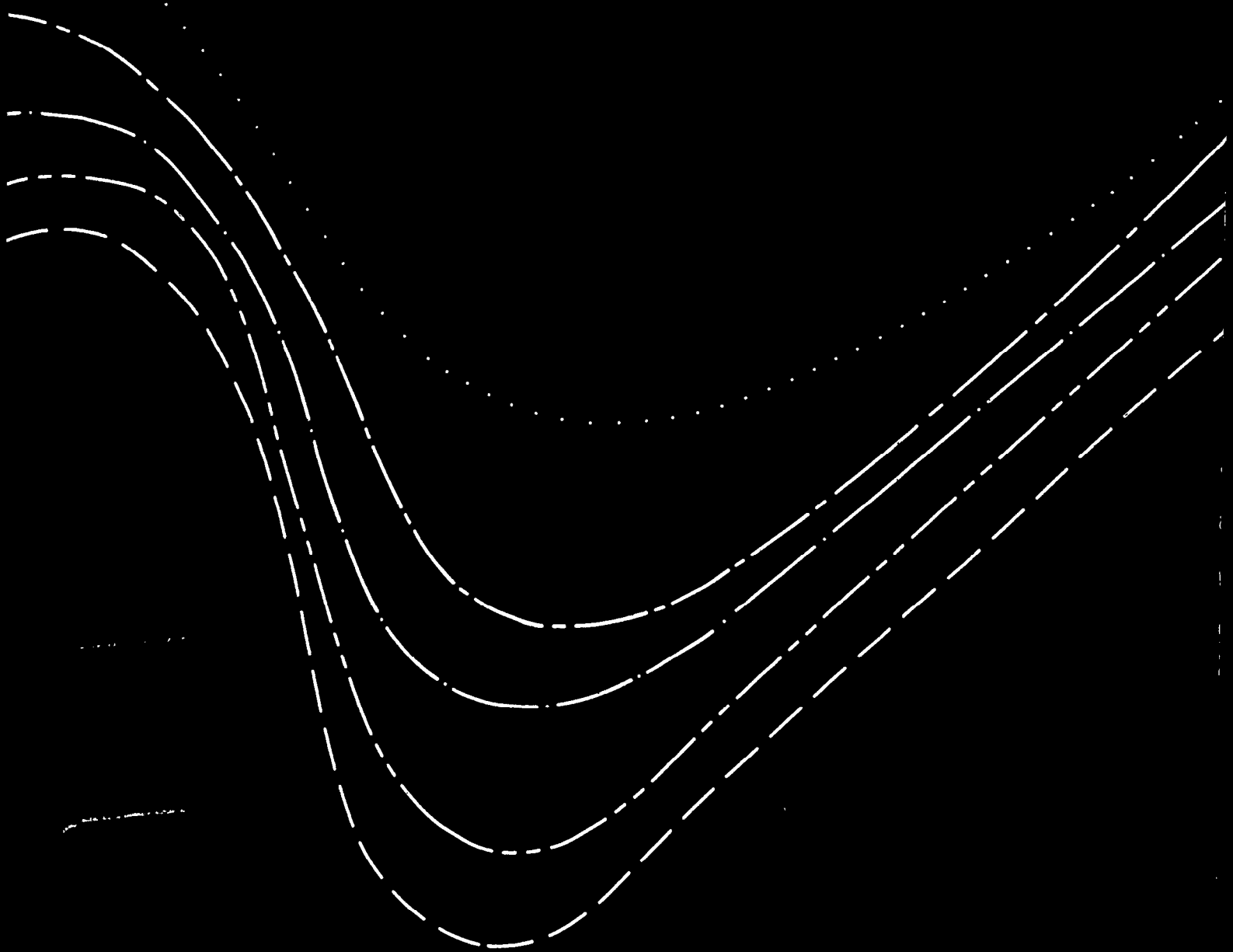

Prepared by the
U.S. GEOLOGICAL SURVEY

in cooperation with the
TENNESSEE DEPARTMENT OF TRANSPORTATION

Hupp, 1986a; Simon, 1989). Because the approach of this study was dictated to some extent by the results of previous work in West Tennessee, a fairly detailed review of those studies will follow in a later section.

Vegetation Response

Vegetation analyses (dendrochronological and plant ecological) are an integral part of the present study. The use of vegetation analyses in the interpretation of geomorphic disturbances, is a relatively recent activity (Graf, 1977; White, 1979: Cairns, 1980; Hupp, 1988). Only a few analyses of riparian vegetation along channelized streams have been conducted (McCall and Knox, 1978; Shields and Nunnally, 1985; Simon and Hupp, 1986a; 1986b; Hupp, 1987).

All of the above-mentioned studies of vegetative response rely on certain basic dendrochronologic concepts that are based on the annual-growth increment of woody plants--the tree ring. Hydrogeomorphic events such as floods and bank failures usually affect the growth rate of woody plants such that datable anomalies can be detected in wood tissue. These anomalies include corrasion scars, tilt sprouts, eccentric growth rings, and suppression or release sequences. Thus, by coring or taking cross-sections of affected stems and counting the number of growth rings since the plant was affected, the number of years since the event occurred can be determined. These techniques have been used in West Tennessee to obtain rates of channel widening and bank accretion (Hupp and Simon, 1986; Hupp, 1987) and to determine the date of initial bank stability.

The magnitude and timing of geomorphic processes are reflected in the presence and character of riparian plants along modified channels or along channels upstream from modifications. Vegetation can be virtually absent along unstable reaches, whereas dense thickets of black willow, river birch, or silver maple can dominate in stable reaches (Hupp and Simon, 1986). The degree of revegetation on the channels banks has been used as an indicator of the general stage of bank-slope development (Simon and Hupp, 1986a, and Simon, 1989).

Examples From West Tennessee Studies

System-wide channel adjustments along streams in West Tennessee have been studied since 1983 by the U.S. Geological Survey. These adjustments involve drastic changes to both the channel bed and banks.

Channel Bed-Level Adjustments

The general form given by Simon and Hupp (1986a) and used to describe bed-level adjustments through time is:

$$E = a(t)^b \quad (2)$$

where E = elevation of the channel bed for a given year, in feet above sea level;
a = coefficient determined by regression, representing the premodified elevation of the channel bed, in feet above sea level;
t = time since beginning of adjustment process, in years, where $t_o = -1.0$ (year prior to onset of adjustment process); and
b = dimensionless exponent, determined by regression and indicative of the nonlinear rate of change on the channel bed.

The power function was used because it consistently provided better fits to the measured data than an exponential function. The exponential function, although having a greater physical basis, did not mirror the measured data well when "t" was small. Discussions regarding observed and predicted values using the power function are given in Simon (in press).

Trends of channel bed-level change through time at stream gaging stations (where bed elevation is measured every 4 to 6 weeks) having periods of record of up to 20 years were analyzed by regression of equation 2 and by using a mean channel-bed elevation for each year. Derived trends supported the concept of nonlinear bed-level adjustment (fig. 3). Once it was established that power functions provided the best fit to this gaged data, data from periodically surveyed sites were similarly fitted. Sites with just two recorded channel-bed elevations were included because of confidence in the general trend of adjustment at a site, and to increase areal coverage of the data network.

In situations where disturbed reaches undergo an initial phase of general degradation (-b), followed by a period of general aggradation (+b), the data set was divided into separate degradation and aggradation periods. The separate data sets were then analyzed by regression using equation 2. The curve of the relation described by equation 2 shows that the rate of channel bed-level adjustment at a site is initially rapid and then diminishes with time as the slope of the curve becomes very flat. Values of b calculated in this and previous studies are listed by stream in table 3.

A bed-level model developed by (Simon, 1989) is summarized using the Obion River system as an example (fig. 4). Maximum rates of degradation (largest negative b-values) occur along the stream reach just upstream from the area of maximum channel disturbance (AMD; near river mile 68), which is labeled A in figure 4, as a response to the significant increase in stream power imposed by the

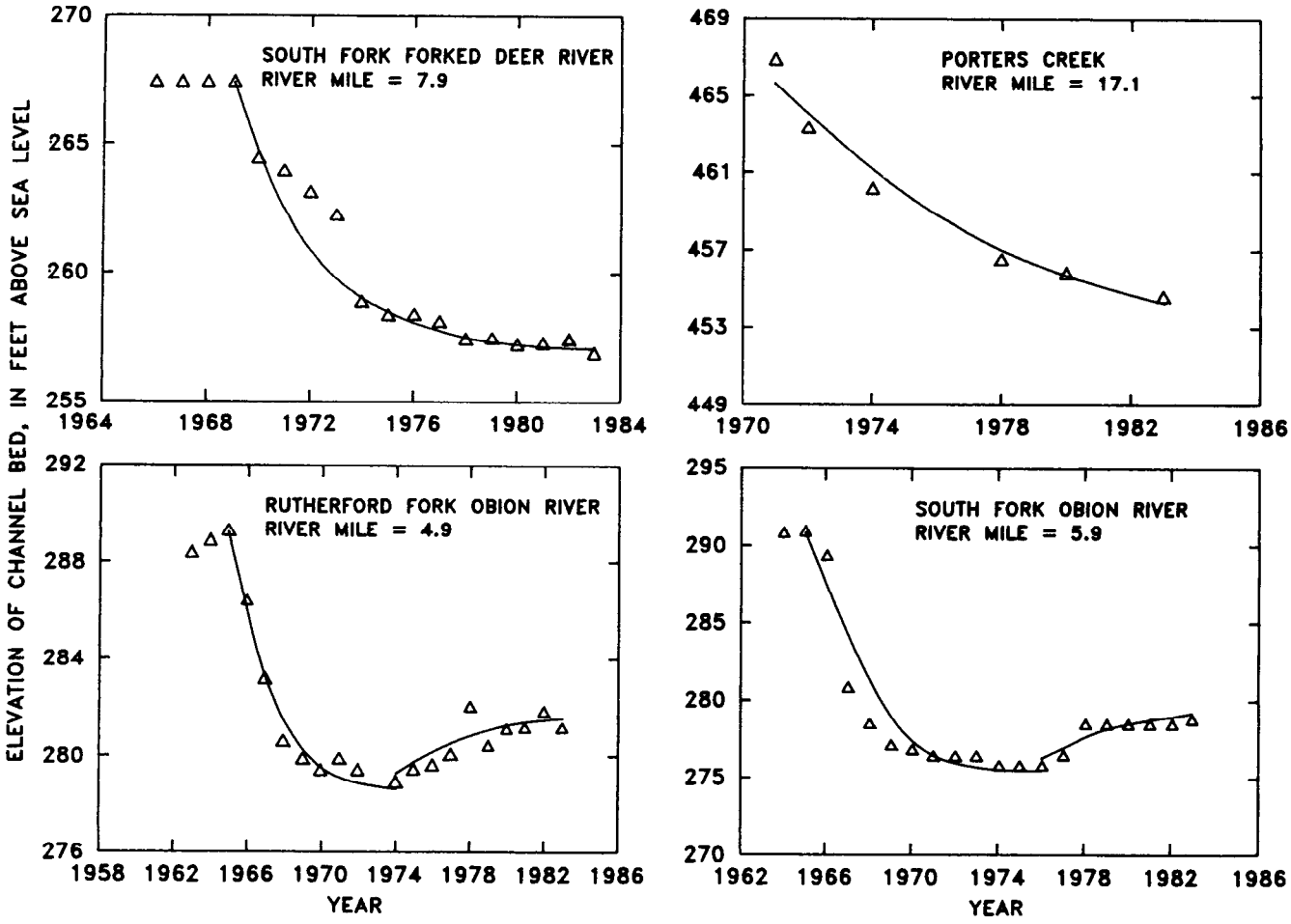

Figure 3.--Relation of channel-bed elevation and time since channel modification for selected stream sites in West Tennessee (curves are visually fitted). (Modified from Simon, 1989.)

channel work here in 1967. The effect of this degradation is to reduce channel gradient (Simon and Robbins, 1987). Degradation rates decrease nonlinearly with distance upstream (curve C in fig. 4). Curve C also represents the headward migration of the degradation process and therefore has a temporal (t_o in table 3), as well as spatial component. Channel-bed degradation continues for 10 to 15 years at sites just upstream from the AMD. The effect of the channel modifications on upstream channel beds decreases with distance, resulting in minimal degradation rates at about river mile 94 (b = 0.0) This is analogous to Bull's (1979) threshold of critical stream power. Further upstream (E in fig. 4), the channel beds of the Obion River system (including upstream reaches of the North, South, and Rutherford Forks) are unaffected by the downstream channel modifications; reaches aggrade at "background" rates (b= 0.003 to 0.006).

Table 3.--*Indicator of nonlinear rates of aggradation and degradation (b values)*

[b=indicator of nonlinear gradation rate; n=number of observations; r^2=coefficient of determination, and are provided for gaged stations only to provide a measure of data scatter; RM=river mile, add 62.4 miles to value for sites on Hoosier Creek and the Obion River forks to match with figure 4; t_0=year prior to beginning of gradation process; *=specific gage data used; --=not applicable; b values column=calculated from equation 2 ($E = a(t)^b$), page 15]

Stream	Station number	b	n	r^2	RM	t_0
Cane Creek	07300025	-0.00989	6	--	16.53	1969
	07300022	-0.00930	6	--	15.95	1969
	07300020	-0.00560	6	--	15.36	1969
	07300019	-0.01060	6	--	14.83	1969
	07300018	-0.01430	6	--	14.05	1969
	07300017	-0.01660	6	--	13.39	1969
	07300016	-0.01540	6	--	12.59	1969
	07300015	-0.01620	6	--	11.84	1969
	07300014	-0.02020	6	--	11.31	1969
	07300013	-0.02330	6	--	11.05	1969
	07300012	-0.02300	6	--	10.26	1969
	07300011	-0.02470	6	--	9.92	1969
	07300010	-0.02210	6	--	8.98	1969
	07300009	-0.03140	6	--	7.99	1969
	07300008	-0.03090	6	--	7.06	1969
	07300007	-0.02960	6	--	6.19	1969
	07300006	-0.02860	6	--	5.71	1969
	07030005	-0.02780	6	--	4.06	1969
	07300004	-0.02730	6	--	3.6	1969
	07300003	-0.01660	6	--	2.52	1969
	07300002	-0.01480	6	--	1.95	1969
	07300001	-0.01480	6	--	0.61	1969
Cub Creek	07029447	-0.00243	3	--	6.92	1969
	07029448	-0.00342	3	--	5.73	1969
	07029449	-0.00565	4	--	2.16	1969
	07029450	-0.00905	5	--	1.54	1969
	07029450	0.00272	2	--	1.54	1976
Hoosier Creek	07025660	-0.00843	3	--	5.15	1967
	07025666	-0.01130	4	--	2.99	1966
	07025690	-0.02081	3	--	0.55	1965

Table 3.--*Indicator of nonlinear rates of aggradation and degradation (b values)*--Continued

Stream	Station number	b	n	r^2	RM	t_o
Hoosier Creek	07025690	0.00274	2	--	0.55	1968
	07025691	-0.02630	3	--	0.01	1965
Hyde Creek	07030007	-0.00737	2	--	2.37	1969
	07030004	-0.01070	4	--	1.38	1969
	07030002	-0.01380	3	--	0.74	1969
	07030001	-0.02050	4	--	0.01	1969
North Fork Forked Deer River.	07028500	0.02370	16	0.92	34.60	1954*
	07028820	-0.00740	4	--	23.90	1977
	07028835	-0.01076	5	--	20.18	1974
	07028840	-0.00839	4	--	18.82	1978
	07029100	-0.01720	10	0.95	5.30	1973*
	07029105	-0.02297	3	--	3.83	1972
	07029105	0.01024	6	--	3.83	1979
North Fork Obion River.	07025320	0.0011	15	0.69	36.90	1969*
	07025340	-0.00206	2	--	26.40	1979
	07025375	-0.00490	2	--	21.10	1975
	07025400	-0.00372	13	0.80	18.00	1972*
	07025500	-0.01240	6	0.93	9.84	1965*
	07025600	-0.02470	4	0.85	5.90	1965*
	07025600	0.00303	5	0.89	5.90	1967*
Obion River	07024800	-0.02220	10	0.95	68.50	1965*
	07024800	0.00463	10	0.74	68.50	1974*
	07025900	-0.04030	4	0.81	62.20	1965*
	07025900	0.00235	16	0.76	62.20	1968*
	07026000	0.00908	19	0.93	53.70	1965*
	07026300	0.00518	15	0.84	34.20	1963*
	07027200	0.00585	16	0.74	20.80	1960*
Pond Creek	07029060	-0.00828	5	--	11.37	1977
	07029065	-0.00799	4	--	9.82	1977
	07029070	-0.01233	4	--	7.32	1977
	07027080	-0.00900	5	--	1.06	1977
Porters Creek	07029437	-0.01069	7	--	17.10	1971
	07029439	-0.01320	7	--	11.20	1971
	07029440	-0.00578	6	--	8.89	1971
Rutherford Fork Obion River.	07024900	0.00149	19	0.60	29.90	1969*

Table 3.--*Indicator of nonlinear rates of aggradation and degradation (b values)*--Continued

Stream	Station number	b	n	r^2	RM	t_o
Rutherford Fork	07025000	-0.00317	4	--	17.90	1977
Obion River.	07025025	-0.00493	3	--	15.20	1977
	07025050	-0.00991	4	--	10.40	1972
	07025050	0.00356	4	--	10.40	1977
	07025100	-0.01728	9	0.93	4.90	1965*
	07025100	0.00433	9	0.88	4.90	1974*
South Fork Forked	07027720	-0.00895	6	--	27.60	1976
Deer River.	07027800	-0.00950	10	0.92	16.30	1974*
	07028000	-0.00978	5	--	13.30	1969
	07028050	-0.01264	5	--	11.90	1969
	07028100	-0.01630	15	0.94	7.90	1969*
	07028200	0.01180	13	0.92	3.30	1969*
South Fork Obion	07024800	-0.02430	11	0.87	5.80	1965*
River.	07024800	0.00544	9	0.88	5.80	1975*
	07024300	0.00030	25	0.07	38.50	1963*
	07024350	0.00133	13	0.90	34.40	1969*
	07024430	-0.00054	4	--	28.40	1972
	07024460	-0.00238	6	--	23.20	1972
	07024500	-0.00661	7	0.90	19.20	1977*
	07024525	-0.00573	5	--	16.80	1972
	07024550	-0.00932	4	--	11.40	1972
Hatchie River	07030050	0.00310	18	0.85	33.30	1964*
	07029500	0.00100	19	0.52	135.1	1964*
Wolf River	07031650	-0.00560	5	--	18.90	1969
	07030500	0.00060	13	0.50	44.40	1972*

Sites downstream from the AMD (line B in fig. 4) aggrade immediately after channel modification with material delivered from eroding reaches upstream. Aggradation (near 'D', but upstream of the AMD, in fig. 4) occurs at previously degraded sites where gradient has been significantly reduced by incision and knickpoint migration. Flows become incapable of transporting the greater bed-material loads being generated from upstream channel beds. The channel therefore aggrades (according to eq. 1) and increases gradient and transporting capacity. This "secondary aggradation" migrates headward with time and is apparently a response to excessive lowering (overadjustment) by the degradation phase (Simon, in press). This represents the first of a possible series of channel-bed degradation and aggradation oscillations (Simon, in press). Hey (1979) and Alexander (1981) similarly argue for alternating phases of degradation and aggradation following rejuvenation of an alluvial channel. Thus,

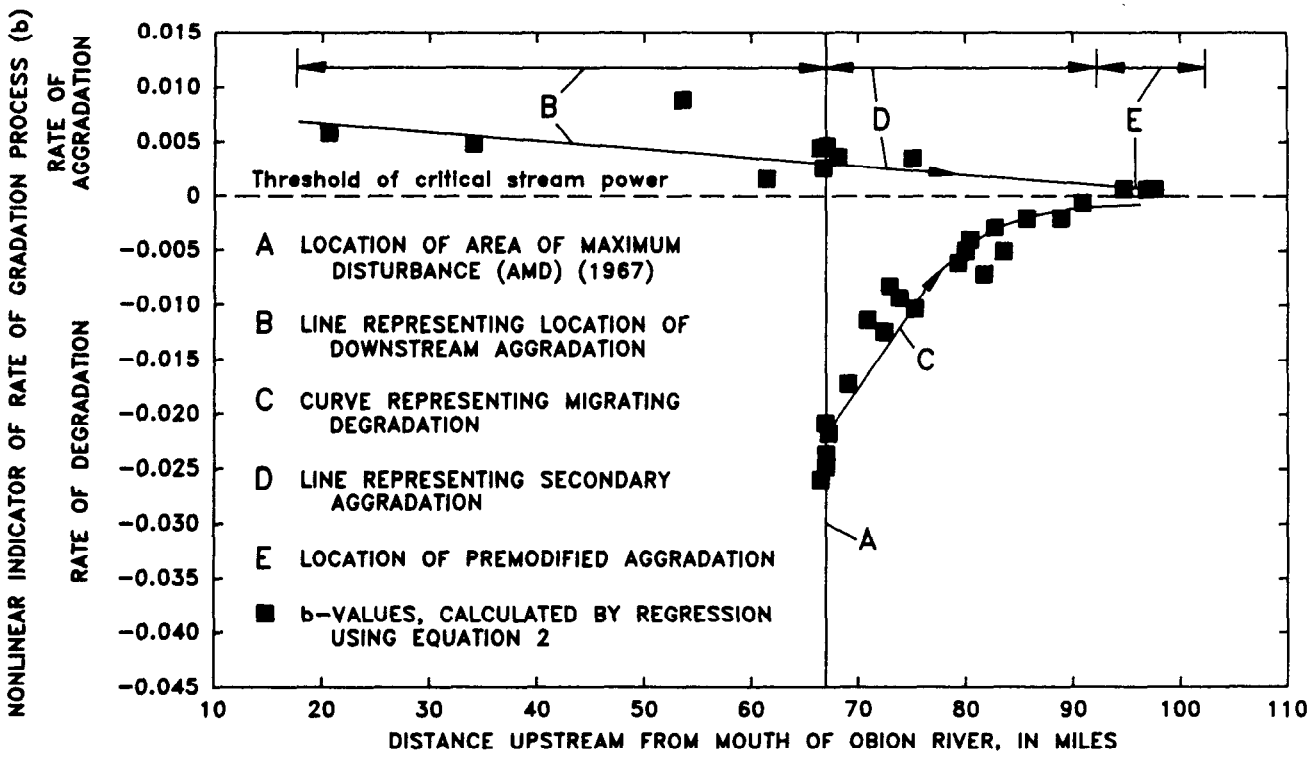

Figure 4.--Model of channel bed-level response to channel disturbance in the Obion River system.

channel bed-level adjustment does follow nonlinear trends, both over time at a site (fig. 3), and over time with distance upstream (fig. 4).

Lateral Adjustments

Previous studies in West Tennessee concentrated on the role of channel degradation in instigating bank instabilities and channel widening. Simon (in press) found a direct relation between the amount of channel bed-level lowering and subsequent widening. By combining the bed-adjustment model with observed morphologic changes on the channel banks, and by substituting observed morphologic changes that were occurring over space as changes over time, conceptual models of bank-slope development and channel evolution were developed (tables 4 and 5). Dominant channel processes were used to differentiate the six-stages in these models.

Three dynamic surfaces were identified on the channel banks and are outlined in table 4: vertical face, upper bank, and slough line (Simon and Hupp, 1986a, b; fig. 5). The vertical face and upper bank are located on the upper two-thirds of the bank and represent the location of the failure plane and the failed material. The slough line, representing the location of initial bank stability, forms during the

Table 4.--*Stages of bank-slope development*

[-- = not applicable; AMD = area of maximum disturbance]

Stage No.	Stage Name	Bed-level adjustment type	Location in network	Process on channel bed	Active widening	Failure types	Bank surfaces present	Approximate bank angle, in degrees
I	Premodified	Premodified	Upstream-most reaches.	Transport of sediment or mild aggradation.	No	--	--	20-30
II	Constructed	--	Where applicable.	Dredging	By man	--	--	18-34
III	Degradation	Migrating degradation.	Upstream from the AMD.	Degradation	No	--	--	20-30
IV	Threshold	Migrating degradation.	Close to the AMD.	Degradation	Yes	Rotational, slab, pop-out.	Vertical face upper bank.	70-90 25-50
V	Aggradation	Secondary aggradation.	Upstream of the AMD.	Aggradation	Yes	Rotational, slab, pop-out, low-angle slides.	Vertical face upper bank slough line.	70-90 25-40 20-25
VI	Restabilization	Downstream-imposed aggradation.	Downstream of the AMD.	Aggradation	No	Low-angle slides, pop-out.	Vertical face upper bank slough line.	70-90 25-35 15-20

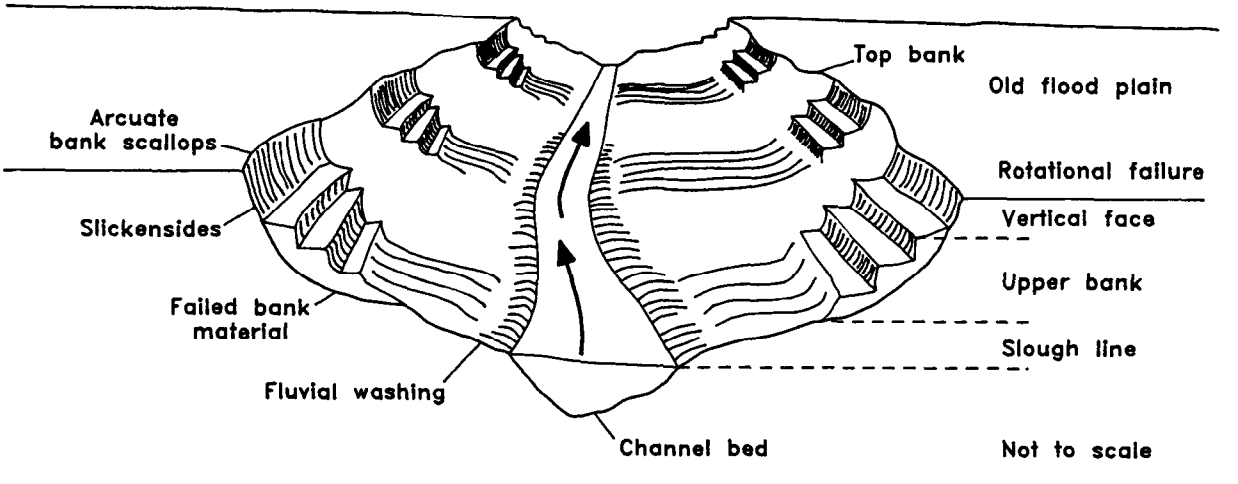

Figure 5.--Generalized streambank section showing typical geomorphic surfaces.

Table 5.--*Stages of channel evolution*

[-- = not applicable]

Stage No.	Stage Name	Dominant processes: Fluvial	Dominant processes: Bankslope	Characteristic forms	Geobotanical evidence
I	Premodified	Sediment transport, mild-aggradation; basal erosion on outside bends; deposition on inside bends.	--	Stable, alternate bars, convex, top-bank shape; flow-line high relative to top bank; channel straight or meandering.	Vegetated banks to flow-line.
II	Constructed	--	--	Trapezoidal cross section linear bank surfaces; flow-line lower relative to top bank.	Removal of vegetation (?).
III	Degradation	Degradation; basal erosion on banks.	Pop-out failures	Heightened and steepended stream banks; alternate bars eroded; flow-line lower relative to top bank.	Riparian vegetation high relative to flow-line and may lean to channel.
IV	Threshold	Degradation; basal erosion on banks.	Slab, rotational and pop-out failures.	Large scallops and bank retreat; vertical-face and upper-bank surfaces; failure block on upper bank; some reduction in bank angles; flow-line very low relative to top bank.	Tilted and fallen riparian vegetation.
V	Aggradation	Aggradation; development of meandering thalweg; initial deposition of alternate bars; reworking of failed material on lower banks.	Slab, rotational and pop-out failures; low-angle slides of previously failed material.	Large scallops and bank retreat; vertical face upper bank, and slough line; flattened bank angles; flow line low relative to top bank; development of new flood plain (?).	Tilted and fallen vegetation; re-establishing vegetation on bank; deposition of material on root collars of slough-line vegetation.
VI	Restabilization	Aggradation; further development of meandering thalweg, further deposition of alternate bars; re-working of failed material; some basal erosion of outside bends.	Low-angle slides; some pop-out failures near flow line.	Stable, alternate channel bars; Convex-short vertical face at top bank; flattened bank angles, development of new flood plain (?); flow-line high relative to top bank. flow-line high relative to top bank.	Re-establishing vegetation extends up slough-line and upper-bank; deposition of material above root collars slough-line and upper-bank vegetation; vegetation establishing on bars.

aggradation stage (stage V) from colluvium moving further down slope under saturated conditions, and by the deposition of fluvial sediments. Woody vegetation becomes established on the slough line and can be dated by dendrochronologic techniques to establish the timing of lower bank stability (Hupp, 1987). A simplified summary of the types of geobotanical evidence used to aid in differentiating among stages of channel evolution is given in table 5 (Simon, 1989).

Certain species are useful as surrogate indicators of the physical conditions associated with a particular site. The presence of any established woody plants on "affected" banks suggests some bank

stability. After initial stabilization pioneer vegetation becomes established and increasingly more complex vegetation assemblages grow on these previously disturbed banks. Thus, progressive suites of vegetation are indicators of increasingly stable bank conditions (Hupp, 1987).

METHODS OF INVESTIGATION

The methods used in this study are interdisciplinary. They include the fields of geomorphology, soil mechanics and geotechnical engineering, hydrology, dendrochronology, and ecology. A total of 105 sites were used.

Site Selection

The streams studied reflect varying magnitudes and types of channel modifications from 1959 through the 1970's (table 2). A sufficient number of sites was selected along each stream system to assess adjustment trends and processes and to develop quantitative relations with distance upstream (fig. 6 and table 6). At least two previous channel cross sections (a premodified cross section and the constructed cross section) were used to analyze adjustment trends. An attempt was also made to include channels representative of the various geologic formations that crop out in the region (table 1). Because all of the study sites are near bridges, particular caution was used to avoid channel sections that reflected a strong hydraulic influence by the bridge. In most cases, cross sections were surveyed away from the hydraulic influence of the bridge structure and fill materials.

Data Collection, Compilation, and Analysis

Channel-geometry measurements were made from 1983 through 1987 at the sites indicated in table 6 as part of this and previous studies. These data were combined with previously assembled data sets (Simon, in press).

Channel Morphology

Channel-geometry data were used to determine amounts of morphologic change and to trace channel evolution over time and space. Data included channel-bed (thalweg) elevation, channel width, bank angles, bank height, and classification of various geomorphic surfaces.

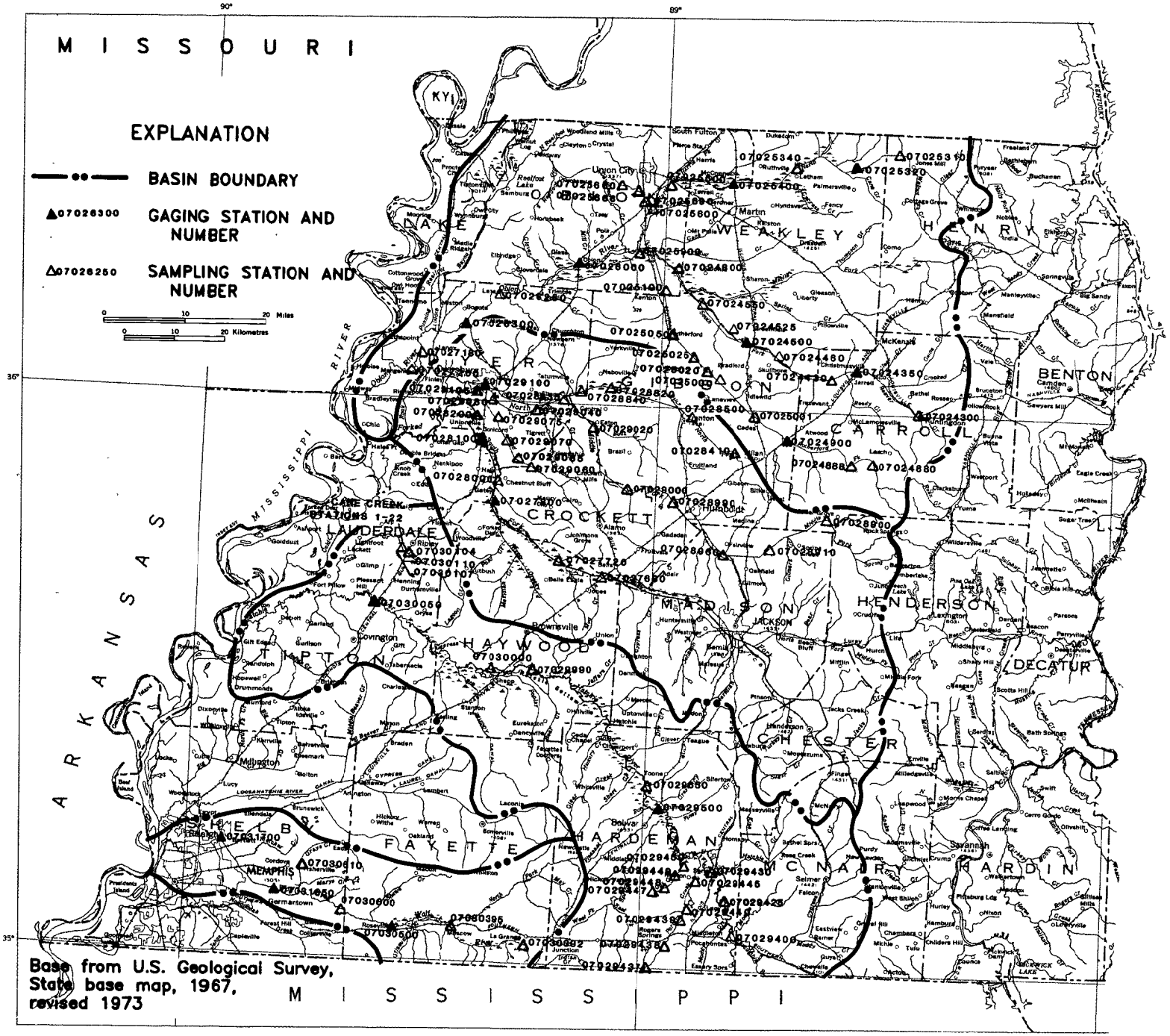

Figure 6.—Location of sites in study area.

Table 6.--*Summary of data collected at study sites*

[b=indicator of nonlinear gradation rate; BST=shear strength testing]

Stream	Station number	River mile	b	Cross section	BST	Dendro-geomor-phology	Modified channel?
			Obion River Basin				
Obion River	07027200	20.8	X	X	X	X	Yes
	07027180	25.6		X	X	X	Yes
	07026300	34.2	X	X	X	X	Yes
	07026250	42.4		X	X	X	Yes
	07026000	53.7	X	X	X	X	Yes
	07025900	62.2	X	X	X	X	Yes
	07024800	68.5	X	X	X	X	Yes
South Fork Obion River.	07024800	5.8	X	X	X	X	Yes
	07024550	11.4	X	X	X	X	No
	07024525	16.8	X	X	X	X	No
	07024500	19.2	X	X	X	X	No
	07024460	23.2	X	X	X	X	No
	07024430	28.5	X	X	X	X	No
	07024350	33.8	X	X		X	No
Rutherford Fork Obion River.	07025100	4.9	X	X	X	X	Yes
	07025050	10.4	X	X	X	X	No
	07025025	15.2	X	X	X	X	No
	07025020	17.1		X	X	X	No
	07025001	24.5				X	No
	07025000	17.9	X	X	X	X	No
	07024900	29.9	X	X	X	X	No
	07024888	39.4			X	X	No
North Fork Obion River.	07025600	5.9	X	X	X	X	Yes
	07025500	10.0	X	X	X	X	Yes
	07025400	18.0	X	X	X	X	No
	07025375	21.1	X	X	X	X	No
	07025340	26.4	X	X	X	X	No
	07025320	34.9	X	X	X	X	No
Hoosier Creek	07025690	0.55	X	X	X		Yes
	07025666	2.99	X	X	X		Yes
	07025660	5.15	X	X	X		Yes
			Forked Deer River Basin				
North Fork Forked Deer River.	07029105	3.83	X	X	X	X	Yes
	07029100	5.30	X	X	X	X	Yes
	07029040	13.55		X	X	X	No
	07028840	18.82	X	X	X	X	No
	07028835	20.18	X	X	X	X	No
	07028820	23.9	X	X	X	X	No
	07028500	34.6	X	X	X	X	No
	07028410	39.6		X		X	No

Table 6.--*Summary of data collected at study sites*--Continued

Stream	Station number	River mile	b	Cross section	BST	Dendro-geomor-phology	Modified channel?
			Forked Deer River Basin--Continued				
South Fork Forked Deer River.	07028200	3.3	X	X	X	X	Yes
	07028100	7.9	X	X	X	X	No
	07028050	11.9	X	X	X	X	No
	07028000	13.3	X	X	X	X	No
	07027800	16.3	X	X	X	X	No
	07027720	27.6	X	X	X	X	No
	07027680	33.7		X	X	X	No
Middle Fork Forked Deer River.	07029020	5.2		X		X	No
	07029000	14.6		X		X	No
	07028990	21.5		X		X	No
	07028900	44.9		X		X	No
	07028960	30.5		X		X	No
	07028910	37.0		X		X	No
Pond Creek	07029080	1.1	X	X	X	X	No
	07029075	3.1		X	X	X	No
	07029070	7.3	X	X	X	X	No
	07029065	9.8	X	X	X	X	No
	07029060	11.4	X	X	X	X	No
			Hatchie River Basin				
Hatchie River	07030050	33.3	X			X	No
	07030000	68.4				X	No
	07029650	121.1				X	No
	07029500	135.1	X			X	No
	07029430	162.3				X	No
	00029400	181.8				X	No
	07029270	200.1					No
Cane Creek	1	.61	X	X	X	X	Yes
	2	1.95	X	X	X	X	Yes
	3	2.52	X	X	X	X	Yes
	4	3.64	X	X	X	X	Yes
	5	4.02	X	X	X	X	Yes
	6	5.72	X	X	X	X	Yes
	7	6.27	X	X	X	X	Yes
	8	7.06	X	X	X	X	Yes
	9	7.99	X	X	X	X	Yes
	10	8.99	X	X	X	X	Yes

Table 6.--*Summary of data collected at study sites*--Continued

Stream	Station number	River mile	b	Cross section	BST	Dendro-geomor-phology	Modified channel?
			Hatchie River Basin--Continued				
Cane Creek	11	9.92	X	X		X	Yes
	12	10.25	X	X	X	X	Yes
	13	11.05	X	X		X	Yes
	14	11.36	X	X	X	X	Yes
	15	11.84	X	X		X	Yes
	16	12.58	X	X	X	X	Yes
	17	13.39	X	X		X	Yes
	18	13.98	X	X	X	X	Yes
	19	14.85	X	X	X	X	Yes
	20	15.34	X	X	X	X	Yes
	22	15.95	X	X		X	Yes
Hyde Creek	1	0.15	X	X	X	X	Yes
	2	1.21	X	X	X	X	Yes
	4	1.9	X	X	X	X	Yes
Porters Creek	07029445	4.5		X	X	X	Yes
	07029440	8.9	X	X	X	X	Yes
	07029439	11.2	X	X	X	X	Yes
	07029438	13.9		X		X	Yes
	07029437	17.1	X	X	X	X	Yes
Cub Creek	07029450	1.5	X	X	X	X	Yes
	07029449	2.2	X	X		X	Yes
	07029448	5.7	X	X	X	X	Yes
	07029447	6.9	X	X	X	X	No
			Wolf River Basin				
Wolf River	07031700	9.1			X	X	Yes
	07031660	15.4		X		X	Yes
	07031650	18.9	X	X	X	X	Yes
	07030610	23.6		X	X	X	No
	07030600	31.2		X	X	X	No
	07030500	44.4	X	X	X	X	No
	07030395	57.5		X	X	X	No
	07030392	69.9				X	No

Channel-Bed Elevations

The average annual water-surface elevation at a given low-flow discharge can be used to infer an average annual channel-bed level by assuming that changes in water-surface elevation at that discharge are caused by bed-level changes (Blench, 1973). This technique was used at gaged sites to determine average annual changes in channel-bed level because historic bed-elevation data were not available. A low-flow discharge was used to minimize the effect of variations in channel width on flow depth. At all ungaged sites, channel-bed elevation was obtained from surveyed cross sections of the channel (rounded to tenths of feet). Data for premodified and constructed cross sections also were obtained from the U.S. Geological Survey, Corps of Engineers (COE), TDOT, Soil Conservation Service (SCS), and Obion-Forked Deer Basin Authority (OFBA). All ungaged sites were surveyed annually from 1983 to 1987 during low-flow conditions. Channel-bed elevation, if measured in the vicinity of a bridge, is defined for this study as the mean of the minimum nonscoured channel elevations at the upstream and downstream sides of the bridge. The differences between elevations on the upstream and downstream sides generally were insignificant and were used as a reference for assessing the potential hydraulic influence of the bridge.

Changes in bed elevation over time are represented by the parameter "b" (from eq. 2), through a method developed by Simon (1989), and discussed earlier (table 3). Equations derived from the relations such as those shown in figures 4 and 7 are used to estimate changes in bed elevation with time during fluvial adjustment; these rates decrease with distance upstream. Projected amounts of aggradation and degradation are calculated by solving equation 2 for the desired time period using the premodified elevation of the channel bed. Channel-bed elevations for studied streams are calculated at 5-year intervals from 1970 to 2000. If the timing of the start of the adjustment process is unknown, a series of curves can be generated using different starting times (B.A. Bryan, U.S. Geological Survey, written commun., 1987; fig. 8). For example, in figure 8 the differences in the estimated curves are a function of the different starting dates; 1975 and 1981.

Degradation migrates upstream and usually continues for 10 to 15 years at a site in response to channel modifications (Simon and Hupp, 1986a). After 10 to 15 years of degradation at a site, a period of aggradation follows, which also progresses upstream with time. On the basis of analysis of 14 sites in West Tennessee, Simon and Hupp (1986a) report that the aggradation exponent (+b) can be approximated as 0.22 times the degradation exponent (-b) with a standard error (S_e) of 5.8. Data for this analysis are reported in Simon (in press). Therefore, channel-bed elevations over the long term can be estimated. When combined with projected changes in channel width and known flood-plain elevations, channel-bed elevations can be used to estimate future channel geometry. Projections of future channel geometry are provided at the request of TDOT and are intended to be used as general guides.

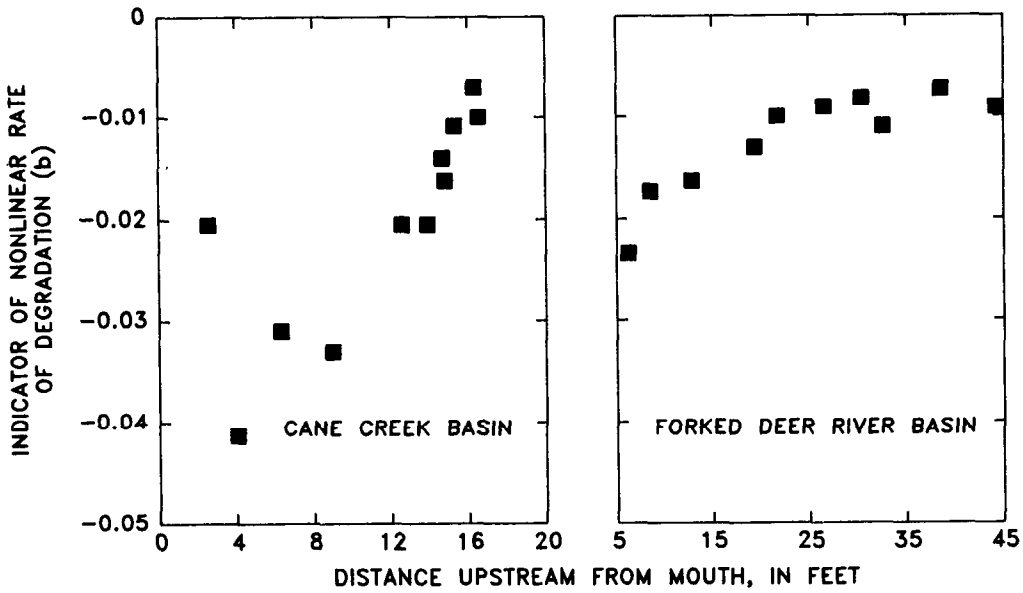

Figure 7.--Bed degradation trends in the Cane Creek and Forked Deer River basins, West Tennessee.

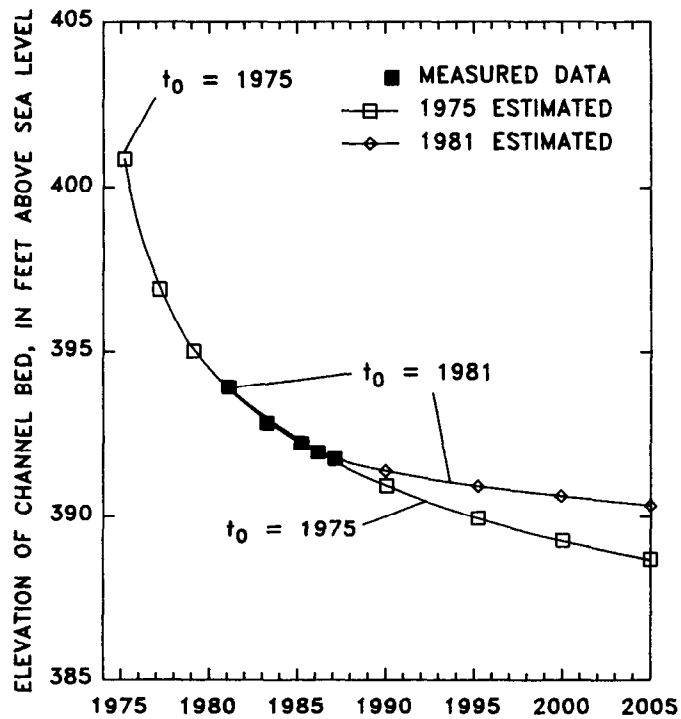

Figure 8.--Example of estimated trends of degradation when time of initial adjustment (t_0) is unknown, Lick Creek, Crockett Co., Tenn. (From B.A. Bryan, U.S. Geological Survey, written commun., 1987.)

Channel Width, Bank Height, and Bank Angles

Unless otherwise noted, channel widths represent top-bank widths as measured from the flood-plain surface. Premodified and constructed were obtained from dredging plans (OFBA, SCS, and COE); subsequent width data were acquired from cross sections measured by the U.S. Geological Survey and, in some cases, from Corps of Engineers and U.S. Geological Survey gaging station records.

Bank height was defined as the difference between the elevation of the flood plain and the elevation of the channel bed. In cases where a man-made levee is an integral part of the bank, bank height is calculated from the top of the levee and represents a maximum height. Bank angles were obtained in one of two ways: they were (1) calculated from available cross-sectional data, or (2) measured during this study. Angles were obtained for the vertical face, upper bank, slough line, and depositional surfaces (fig. 5).

Volumetric Changes in Channel Size

Variation in channel-forming processes during fluvial adjustment causes changes in channel area and morphology through the removal or deposition of materials. By comparing cross sections over the length of a given stream for different time periods, estimates of the volume of material eroded or deposited can be made.

Measured cross sections provided by the COE, OFBA, and SCS were used as the primary data base for documenting changes in channel areas and volumes (table 7). The cross sections cover the period from the mid-1960's through the mid-1980's.

For each cross section (assuming bankfull dimensions) channel area, mean depth, and width were digitized, calculated, and plotted by river mile for each time period. Because cross-sectional data were obtained from a variety of sources, direct section-to-section comparisons were not always possible. Instead a trend line was visually fitted through the data and was used to represent values of a given parameter over the length of the stream, and for the specified period. By overlaying the plots for the specific feature and by digitizing the area between the trend lines, estimates could be made of changes in that feature due to adjustment processes acting between the date of construction (or initial adjustment) and the present date.

The integration of depth changes at a site over the stream length studied provides information regarding the amount of vertical change in square feet. By then multiplying by the bottom width, the volume of material eroded or deposited from the channel bed by fluvial processes can be determined. Because changes in channel width generally occur after significant incision, a constant bottom width was

Table 7.--*Dates of cross-section measurements and data sources used to compute volumes of channel materials eroded or deposited during fluvial adjustment*

Stream	Year	Data source
Obion River mainstem	1963	U.S. Corps of Engineers
	1975	U.S. Corps of Engineers
	1982	U.S. Corps of Engineers
	1983	U.S. Geological Survey
	1987	U.S. Geological Survey
North Fork Obion River	1965	U.S. Corps of Engineers
	1975	Continental Engineering
	1983	U.S. Geological Survey
	1987	U.S. Geological Survey
South Fork Obion River	1965	U.S. Corps of Engineers
	1978	U.S. Corps of Engineers
	1983	U.S. Geological Survey
	1987	U.S. Geological Survey
Rutherford Fork Obion River	1964	U.S. Corps of Engineers
	1978	Continental Engineering
	1979	Continental Engineering
	1983	U.S. Geological Survey
	1987	U.S. Geological Survey
North Fork Forked Deer River	1974	Continental Engineering
	1983	U.S. Geological Survey
	1987	U.S. Geological Survey
South Fork Forked Deer River	1966	U.S. Corps of Engineers
	1975	Continental Engineering
	1979	Continental Engineering
	1985	U.S. Corps of Engineers
	1987	U.S. Geological Survey
Cane Creek	1968	Soil Conservation Service
	1970	Soil Conservation Service
	1985	Soil Conservation Service
	1987	U.S. Geological Survey

used to estimate the volume of material eroded by degradation. Similarly, plots of width changes provide data (in square feet) that is multiplied by bank height to calculate volumes eroded from the channel banks by mass-wasting processes. Plots of changes in total channel area represent total volumes of sediment eroded or deposited in the channel (fig. 9).

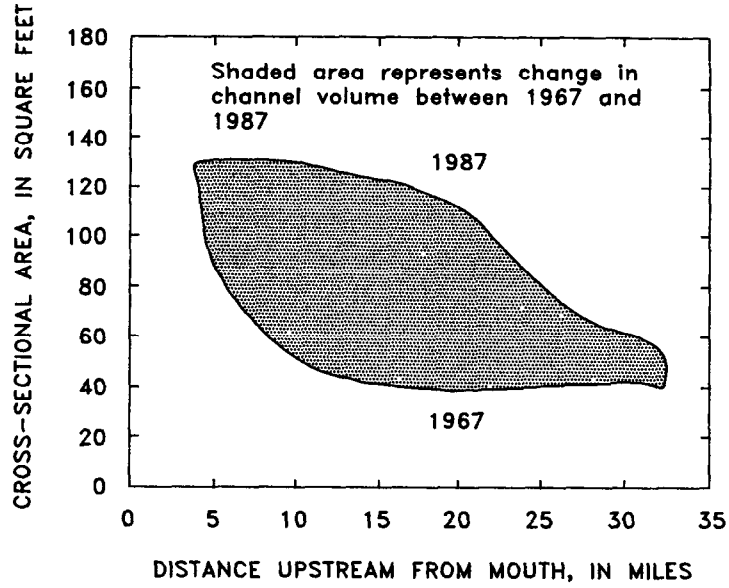

Figure 9.--Idealized example showing determination of change in channel volume using cross-sectional area data.

Geomorphic Surfaces and Stage Identification

The variation in adjustment processes over the course of fluvial recovery from a channel modification results in the formation of specific geomorphic surfaces below the flood-plain level (Simon and Hupp, 1986b; Simon, 1989; and fig. 5). Characteristics of these surfaces such as angles, vegetation, and the presence or absence of bank failures are diagnostic in determining the relative stability of a reach and its stage of channel evolution. The specific geomorphic and botanical attributes of reaches in each of the six stages are summarized in tables 4 and 5. The identification of stage is important in assessing past, present, and future adjustment processes at a site. Field reconnaissance was carried out from 1985 to early 1987 for all sites included in the study (table 6). Data collection involved: (1) locating and dating riparian vegetation on newly stabilized surfaces to determine the timing of initial stability for that surface, and on unstable bank surfaces to estimate rates of bank retreat, (2) noting fluvial undercutting or deposition (bank accretion), (3) noting failure types, block widths and angles, and (4) measuring the height of the banks.

Independent hydrologic characteristics such as flow duration were calculated from mean-daily discharges for gaging stations within the area of study (table 8). The purpose of this was to ascertain (1) the flow durations corresponding to given geomorphic surfaces, and (2) the extent to which the form and development of those surfaces can be related to flow duration.

Elevations (relative to sea level) of the different geomorphic surfaces (vertical face, upper bank, slough line, shelf and bar) were determined from measured cross sections. These elevations were assigned gage-height elevations according to standard gage datums reported by the U.S. Geological Survey and the Corps of Engineers. The water discharge corresponding to that gage height was then

Table 8.--*Streamflow stations and period of record used in flow-duration analysis*

Station name	Station number	Period of record
North Fork Obion River near Martin, Tenn.	07025400	1941-81
North Fork Obion River near Union City, Tenn.	07025500	1931-70
South Fork Obion River near Greenfield, Tenn.	07024500	1931-86
Rutherford Fork Obion River near Milan, Tenn.	07024900	1970-79
Rutherford Fork Obion River near Bradford, Tenn.	07025000	1930-57
Obion River at Obion, Tenn.	07026000	1930-58 1967-86
Obion River near Bogota, Tenn.	07026300	1956-84
North Fork Forked Deer River at Trenton, Tenn.	07028500	1952-71
North Fork Forked Deer River at Dyersburg, Tenn.	07029100	1948-85
South Fork Forked Deer River at Jackson, Tenn.	07027500	1930-73
South Fork Forked Deer River near Gates, Tenn.	07027800	1969-81
South Fork Forked Deer River at Chestnut Bluff, Tenn.	07028000	1930-57
South Fork Forked Deer River near Halls, Tenn.	07028100	1955-83
Beaver Creek at Huntingdon, Tenn.	07024300	1963-86
Hatchie River at Pocahontas, Tenn.	07029400	1942-69
Hatchie River at Bolivar, Tenn.	07029500	1931-86
Hatchie River near Stanton, Tenn.	07030000	1930-58
Hatchie River at Rialto, Tenn.	07030050	1956-79
Wolf River at Rossville, Tenn.	07030500	1931-71
Wolf River at Germantown, Tenn.	07031650	1981-85
Wolf River at Raleigh, Tenn.	07031700	1938-69

obtained from updated rating curves (relation between gage height and discharge) provided by those agencies. By interpolating between points on the flow-duration curve, a flow duration corresponding to the elevation of a given geomorphic surface was obtained.

Differentiation between stages I and VI is based on whether or not a reach has ever been channelized. Stage I reaches generally are sinuous and have not been modified, being represented in this study by the Hatchie River, upstream reaches of the Wolf River and some downstream reaches of the Obion and Forked Deer River forks for the periods prior to any channel work. As in the case of the non-channelized Hatchie River, stage I may encompass long periods of time before abruptly becoming a stage II channel upon construction (such as Cane Creek).

Stage II (constructed) is theoretically an instantaneous condition, followed immediately by either degradation (stage III) or aggradation (stage V), depending on the whether the reach is located upstream or downstream of the AMD, respectively (Simon, 1989). Degradation spans stages III and IV, lasts for 10 to 15 years, and is represented by reaches upstream of the AMD. Maximum rates of degradation occur during stage III. Stage IV is characterized by the onset of bank failures by mass-wasting processes (table 4).

Stages are V and VI are of long duration and are characterized by aggradation, incipient meandering, and bank failures that bring the channel to a stable configuration. Field evidence indicates that the period required for restabilization may be 50 to 100 years from the onset of aggradation during stage V. Small modification lengths and magnitudes may require less time for restabilization.

Shear Strength and Bank Stability

The relative stability of a channel bank is measured by the factor of safety (FS) which is the ratio of the forces that tend to resist mass movement and the gravitational forces that tend to drive that bank towards failure. To assess the roles of these forces in determining bank stability, shear-strength determinations of the bank material are required. Shear strength can be calculated using the Coulomb equation. For a failure plane of unit width and length, and if there is zero pore-water pressure,

$$s = c + \sigma \tan \phi \qquad (3)$$

where

s = shear strength, in pounds per square foot;
c = cohesion, in pounds per square foot;
σ = normal stress, in pounds per square foot; and
ϕ = angle of internal friction, in degrees.

Also, $$\sigma = W (\cos\theta) \quad (4)$$

where W = weight of the failure block, in pounds per square foot, and
θ = angle of the failure plane, in degrees.

Other required variables for calculating the normal stress, such as bank heights and angles, are determined from field surveys. Soil density is an integral component in the calculation of the weight of the failure block and therefore, slope stability (Grissinger, 1982). Soil density samples were obtained at each shear-test location and depth. From these samples, ambient moisture content was calculated assuming a specific gravity of soil solids of 0.096 lbs/in^3.

Soil-mechanics properties, cohesion, and friction angle were determined from field tests using the Iowa Borehole Shear Test Device (BST). This instrument is used to conduct rapid, in situ, direct-shear tests on the walls of a 3-inch diameter borehole (fig. 10). The BST has a number of analytical features different from conventional, laboratory-conducted triaxial-shear tests:

1. Cohesion and friction angle are evaluated separately;
2. A number of separate trials (5 to 12) on the same sample are run for each test, to produce a single c and ϕ value;
3. Data obtained from the instrument are plotted on site, allowing for repetition if the results are unreasonable; and
4. Tests can be carried out at various depths in the bank to locate weak areas (Thorne and others, 1981).

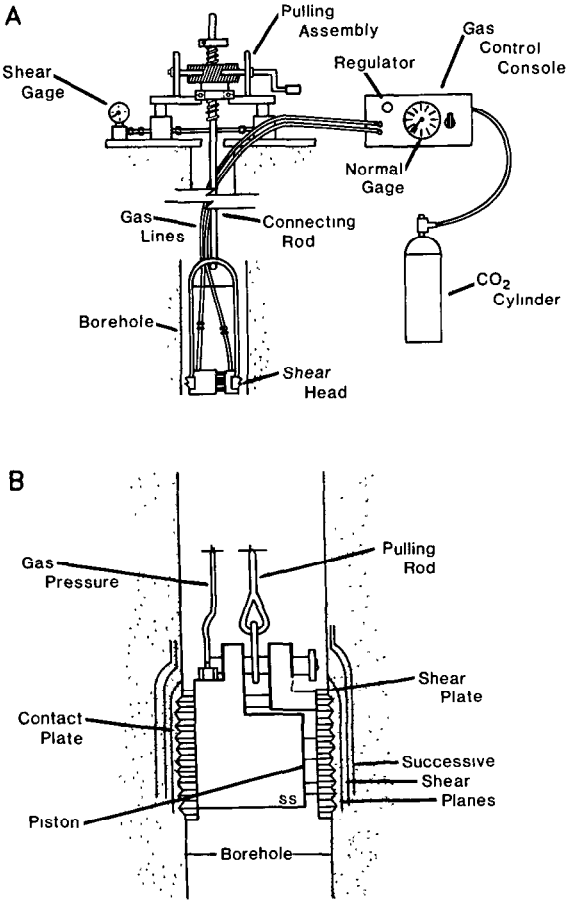

Figure 10.--Schematic drawings of (A) borehole shear-test assembly and (B) detail of shear head in borehole. (Modified from Thorne and others, 1981.)

The BST was introduced by Handy and Fox (1967) as an instrument used to make direct-shear tests on the periphery of a borehole. The BST has seen increasing use following a study by Lohnes and Handy (1968) concerning slope stability in loess

deposits of Iowa and West Tennessee. The instrument has been subsequently used to study a variety of geomorphic processes. Luttenegger and Hallberg (1981) and Thorne and others (1981) provide a review of BST techniques and applications.

The BST was used in the current study because of the project's scope (105 sites) and because it provided the only practical means of acquiring large amounts of shear strength data (168 tests) within the time and budgetary limits of the project. Direct comparison of BST results with more conventional methods such as triaxial shear were well beyond the financial means of the project. Moreover, Lambrechts and Rixner (1981) and Lutenegger (1987) report that the shear-strength determinations made with the BST have the same inherent variability as triaxial shear tests. A good indication of the accuracy of the BST when compared with triaxial data is that the BST achieves ϕ values of +/- 3 degrees and c values of +/- 0.7 pounds per square inch (Wineland, 1975; R. Jacobson, written commun., 1991).

A brief summary of BST operating procedures is given below. The shear head of the BST is lowered into the borehole to the desired depth and expanded under gas pressure to provide the normal force (fig. 10). The soil in contact with the shear head is then allowed to consolidate for at least 10 minutes under the applied normal force. BST tests conducted during this study were considered as drained tests; sufficient consolidation times were used in conjunction with a pore-pressure sensor (mounted on the shear head) to assure that all positive pore pressures were dissipated. Because most soils tested were silts of low plasticity (Simon, in press), and testing was conducted during the summer months, in very few cases were positive pore pressures observed.

The shear head is pulled vertically by means of a pulling assembly located at the surface. The vertical force provides the shearing force on the walls of the borehole and is increased until failure of the soil occurs. Failure is identified by either a decrease in the shearing-force gage or by a constant gage reading over 40 to 50 turns of the pulling assembly (fig. 10). The maximum shearing force, divided by the area of the shear plates represents the shear stress at failure, and when plotted with the corresponding normal stress, produces a point on the Mohr-Coulomb line (fig. 11). Additional trials at increasingly higher normal forces produce a series of points, which by regression, define cohesion (y-intercept) and the angle of internal friction (slope of the line) (fig. 11).

It was found that too short consolidation times resulted in an increased scatter of points, a nonlinear relation between the normal and shear forces, or a flat Mohr-Coulomb failure envelope. In these few cases, the tests were redone with longer consolidation times for each increment of applied normal force.

Drained shear-strength tests were carried out in various materials encountered in the boreholes. Preliminary analysis of COE boring logs indicated relatively homogeneous silt bank materials along all

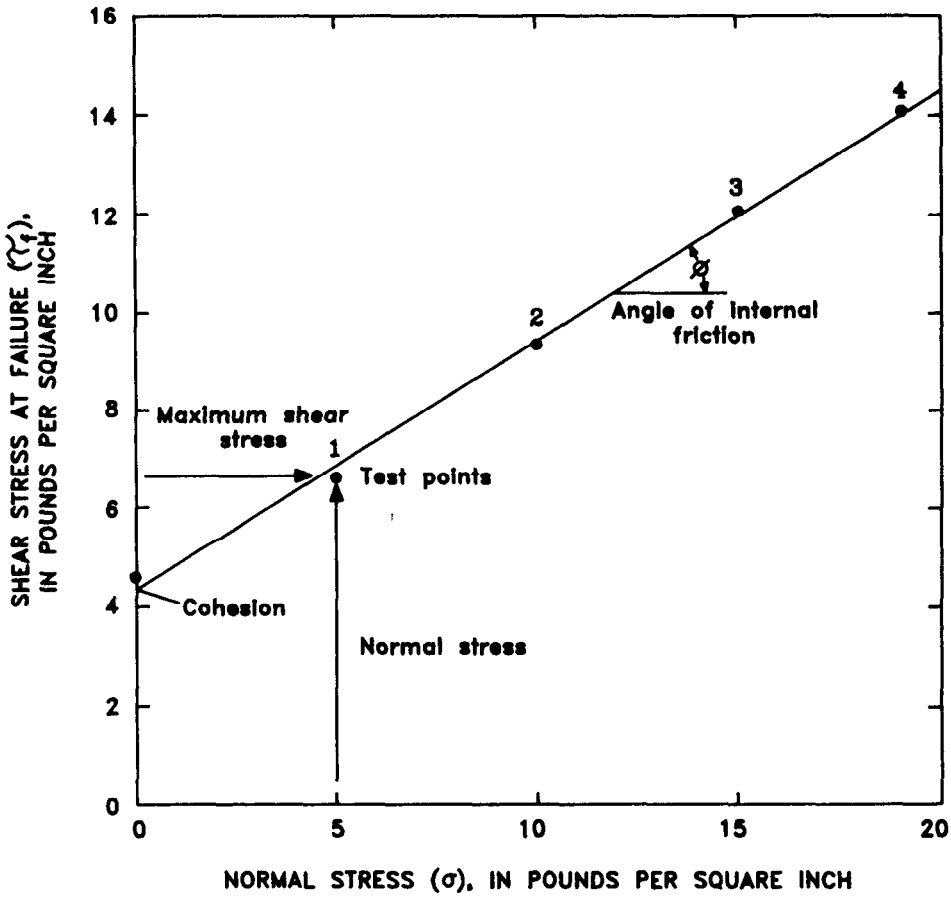

Figure 11.--Idealized relation between normal stress and shear stress (Mohr-Coulomb failure envelope) as derived from borehole shear-test data.

the studied streams. Hand augers were used for holes up to 10-feet deep; mobile drill rigs (supplied by TDOT) were used for tests at greater depths.

At least two tests were performed in fine-grained material (silt-clay) at each site (table 6). Sand-sized materials generally were not tested with the BST because of the absence of cohesion. Angle of internal friction values for these type soils were obtained from the U.S. Bureau of Reclamation (1973). These strata were logged, however, for subsequent use in slope-stability analyses.

Analysis of Bank Stability

The analysis of bank stability may be carried out in a number of ways depending on the assumed shape of the failure surface (planar or curved) and the form of the desired solution (critical conditions or factor of safety).

Factors of safety.--Total-stress analytic solutions for both planar and rotational failures were developed (because of a lack of data on pore pressure) in terms of factors of safety (ratio between the resisting and driving forces). For a planar failure of unit length and width, the factor of safety is:

$$FS = \frac{c + W\cos\theta\tan\phi}{W\sin\theta} \quad (5)$$

and is shown in figure 12. For heterogeneous banks, mean values of c, ϕ, and saturated density (γ_{sat}) were used. The angle of the failure plane was calculated from (Lohnes and Handy, 1968):

$$\tan\theta = \tan\left[\frac{1}{2}i + \frac{1}{2}\phi\right] \quad (6)$$

where i = bank angle, in degrees.

For rotational failures the minimum FS must be determined from a large number of potential-failure "circles". If the circles and failing mass are divided into "k" slices (fig. 13), the factor of safety can be determined by:

$$FS = \frac{\sum_{k=1}^{k=n} c_k + \tan\phi_k}{\sum_{k=1}^{k=n} (W_k \sin\theta_k)} \quad (7)$$

This is a laborious technique, particularly when further complicated by a heterogeneous bank. For these reasons, computer software developed by Huang (1983) was used for the analysis of rotational failures. The program selects the least stable failure surface and is constrained by the elevation of the channel bed (failures are not permitted below this elevation). Required input data include shear-strength properties c, ϕ and γ_{sat} for each soil unit, the configuration of the bank, and the pore-water pressure. Owing to a lack of information on phreatic surfaces and in order to include the effect of pore pressure on calculations of shear strength and factors of safety, a pore-pressure ratio (r_u) is used (Huang, 1983):

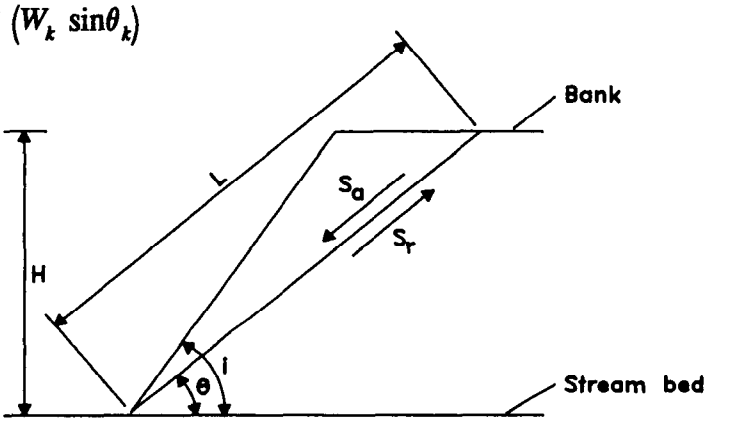

EXPLANATION

H = BANK HEIGHT
L = FAILURE PLANE LENGTH
c = COHESION
ϕ = FRICTION ANGLE
Y = BULK UNIT WEIGHT
i = BANK ANGLE
S_a = Wsinθ (Driving force)
S_r = cL + Ntanϕ (Resisting force)
N = Wcosθ
θ = (0.5i +0.5ϕ) (Failure plane angle)

For the critical case $S_a = S_r$ and :

$$H = \frac{4c \sin i \cos\phi}{Y(1 - \cos[i - \phi])}$$

Figure 12.--Shear failure along a planar slip-surface through the toe. (Modified from Thorne and others, 1981.)

$$r_u = \frac{\textit{volume of failing mass under water x unit weight of water}}{\textit{volume of failing mass in air x unit weight of soil}} \quad (8)$$

Pore-pressure ratios of 0.0 (dry) 0.125, 0.25, 0.375, and 0.50 (saturated) were used to represent the complete range of moisture conditions in this study. The effect of increasing values of r_u is a general decrease in the factor of safety through reduction in the normal-force component by:

$$1 - r_u, \text{ to} \quad (9)$$

$$\sigma = (1-r_u) W \cos \theta \quad (9a)$$

Previous investigations in West Tennessee have shown that mass-bank failures generally occur during or after the recessional limb of storm hydrographs when the bank is still saturated and the support of the flowing water has been removed (Simon, 1989). Bank stability was therefore modeled assuming low-flow elevations in the channel.

Critical-bank conditions.--Critical-bank conditions are defined as the bank angle and height above which failure is expected to occur. This type of analytic solution is desirable for predicting stable-bank configurations on presently unstable banks. Carson and Kirby (1972), defined a dimensionless stability equation of the general form:

$$\frac{\gamma H}{c} = N_s = \textit{function}(\phi, i) \quad (10)$$

where N_S = dimensionless stability number,
H = bank height, and
γ, c, ϕ, i = are as previously defined.

This relation provides information regarding the maximum stable slope in terms of the stability number N_S and i. This analysis was found useful in describing mass-bank failures along degraded streams of northern Mississippi Thorne and others (1981).

Stability charts developed by Chen (1975) were used to calculate critical-bank heights (H_c) by solving equation 10 for a range of bank angles (40 to 90 degrees), and by using ambient, site-specific values of c, ϕ at γ_{sat} (fig. 14). Critical heights for worst-case (saturated) conditions were obtained assuming that ϕ and the frictional component of shear strength goes to 0.0 (Lutton, 1974). Results of solutions of equation 10 for both ambient and worst-case conditions were then plotted on semi-logarithmic paper to produce bank-stability charts like those of Thorne and others (1981) and